

Green Chemistry

Accepted Manuscript



This is an *Accepted Manuscript*, which has been through the Royal Society of Chemistry peer review process and has been accepted for publication.

Accepted Manuscripts are published online shortly after acceptance, before technical editing, formatting and proof reading. Using this free service, authors can make their results available to the community, in citable form, before we publish the edited article. We will replace this *Accepted Manuscript* with the edited and formatted *Advance Article* as soon as it is available.

You can find more information about *Accepted Manuscripts* in the [Information for Authors](#).

Please note that technical editing may introduce minor changes to the text and/or graphics, which may alter content. The journal's standard [Terms & Conditions](#) and the [Ethical guidelines](#) still apply. In no event shall the Royal Society of Chemistry be held responsible for any errors or omissions in this *Accepted Manuscript* or any consequences arising from the use of any information it contains.



Journal Name

ARTICLE

Effective deoxygenation of fatty acids over Ni(OAc)₂ in the absence of H₂ and solvent

Wenjing Li,^{a,b} Yongjun Gao,^a Siyu Yao,^b Ding Ma^{*b} and Ning Yan^{*a}Received 00th January 20xx,
Accepted 00th January 20xx

DOI: 10.1039/x0xx00000x

www.rsc.org/

Different metal acetate salts were systematically examined for the catalytic deoxygenation of stearic acid in the absence of H₂ and solvent for the first time. Ni(OAc)₂ exhibited the highest activity with 62% yield achieved at 350 °C for 4.5 h with only 1 mol% (0.2 wt%) of catalyst. Even with 0.25 mol% (0.05 wt%) catalyst, around 28% yield was achieved within 2 h at 350 °C with 89% selectivity to C17 hydrocarbons. The activity based on C17 yields per Ni was 14.5 mol·mol⁻¹·h⁻¹, considerably higher than previous reports. The catalytically active species were identified to be in situ generated Ni nanoparticles (8–10 nm) formed from the decomposition of the metal precursor with stearic acid as a stabilizer. A new reaction pathway of alkane formation from stearic acid via anhydride intermediate decarbonylation under an inert gas atmosphere was proposed. The excellent stability of catalyst was demonstrated by re-adding substrate to the system, during which the activity remained constant through four consecutive runs. The novel catalytic system was applicable to a range of fatty acids and triglycerides with varying activities.

1. Introduction

The rising concern of the decline of fossil fuel reserves has created increasing interest toward the search for renewable chemicals and fuels for future society, such as the use of lignin, cellulose and chitin for fine chemicals^{1–5} and solar, wind and nuclear energy for fossil fuels replacement. However, the application of solar energy and wind energy is limited by the surrounding environment and nuclear energy suffers from the problems associated with residue disposal and radiation pollution. One of the most suitable renewable sources for future *transportation fuel* are natural oils and fats, derived from such sources as palm, microalgae, jatropha plants and kitchen waste oil, due to their high energy density, structural similarity to fossil fuels (long alkane chain) and as well as the widespread and rich content in nature.^{6–9}

Natural oils and fats are comprised of triglycerides and free fatty acids with a long linear hydrocarbon chain ranging from C4 to C24, in particular C16 and C18.¹⁰ The high viscosity and low volatility of these feedstocks cause severe problems when directly used as fuels in engines such as injector coking, carbon

deposits and lubricant thickening.^{6,11,12} In recent years, much effort has been made to upgrade these renewable sources to biodiesel.^{13–15} Cracking of triglycerides with zeolites can remove the oxygen moieties, but together with a significant portion of carbon loss, causing energy loss.^{16–19} Transesterification of triglycerides with methanol and ethanol using homogenous base catalyzed systems has been commercialized. Unfortunately, the products still contain high oxygen content, so that they are not fully compatible with a diesel engine. To make things worse, this process cannot tolerate high free fatty acid content as acids undergo saponification causing the deactivation of catalysts.^{11,12} Alternatively, the oxygen in triglycerides and free fatty acids can be selectively removed in the form of CO₂, CO or H₂O *via* a deoxygenation process. As such, the feedstock is transformed into liquid hydrocarbons, which are ideal replacements of conventional fossil fuels. Deoxygenation of fatty acids (as model compounds for fats and oils) have been studied with various metal catalysts such as Pd, Pt, Ni, Cu, and W supported on ZrO₂, SiO₂, CeO₂, TiO₂, Al₂O₃, carbon and zeolitic materials under H₂ atmosphere with excellent performance achieved.^{20–29} However, the main disadvantage of this process is the consumption of H₂, which mainly comes from fossil fuels with high costs and difficulties in storage and transportation. Ideally, the fully renewable biofuel needs to be obtained without additional H₂ input. Several reports concerning the deoxygenation process under inert gas or atmospheric conditions have been examined, mainly focused on noble metal catalysts such as Pd^{30–33} and Pt,^{34,35} which are not highly appealing in the industry due to their high cost and low

^a Department of Chemical and Biomolecular Engineering, National University of Singapore, 4 Engineering Drive 4, 117585, Singapore. E-mail: ning.yan@nus.edu.sg; Fax: +65 6779 1936; Phone: +65 6516 2886

^b Beijing National Laboratory for Molecular Sciences, College of Chemistry and Molecular Engineering, Peking University, Beijing 100871, China. E-mail: dma@pku.edu.cn; Fax: +86-10-62758603; Phone: +86-10-62758603

† Electronic Supplementary Information (ESI) available: Details of additional characterizations and reaction optimizations. Supporting Information, Figure S1–S6 and Table S1–3. See DOI: 10.1039/x0xx00000x

abundancy. More recently, Ni based catalysts,³⁶⁻³⁹ after pre-activation with high temperature H₂, were also examined for this deoxygenation process. Most of these reactions were carried out in dodecane, toluene or water, with low activity being observed (for example, 18.1% and 17.8% conversion of stearic acid could be achieved over 60% Ni/SiO₂ and 16% Ni/Al₂O₃ under 300 °C for 6 h, respectively).⁴⁰ New catalytic systems for the deoxygenation of fatty acids/triglycerides in the absence of auxiliary reagent over cheap and easily available metal catalysts are still highly desirable.

In the present study, stearic acid was used as a model compound to identify superior catalyst for the deoxygenation reaction in the absence of solvent and additional H₂. A systematic catalyst screening was carried out over 11 metal acetate salts as pre-catalysts. Ni(OAc)₂ exhibited highest activity with heptadecane and heptadecane as the major products. Different nickel salts were further examined, and Ni(NO₃)₂ and Ni(acac)₂ outperformed NiCl₂ and NiSO₄. In-depth investigations were conducted to identify the real catalytic active species and the reaction pathways. The recyclability and the substrate scope were also evaluated.

2. Experimental

2.1 Materials

Free fatty acids (including stearic acid, palmitic acid, dodecanoic acid, oleic acid and linoleic acid), tristearin, dodecane, Ni(NO₃)₂·6H₂O and Pd(OAc)₂ were purchased from Sigma-Aldrich. [Rh(OAc)₂]₂ and Au(OAc)₃ were purchased from Alfa Aesar. Ni(OAc)₂·4H₂O, Ni(acac)₂, NiCl₂·6H₂O, NaOAc, Ca(OAc)₂·H₂O, Cu(OAc)₂·H₂O, Zn(OAc)₂, Co(OAc)₂·4H₂O, Mn(OAc)₂·4H₂O, AgOAc were purchased from Sinopharm Chemical Reagent (SCR). NiSO₄·6H₂O was purchased from Merck. CH₂Cl₂ was purchased from Fisher and CH₃OH was purchased from Tedia. All chemicals were used without any further purification.

2.2 Reaction setup and analytical techniques

In a typical experiment, stearic acid (200 mg, 0.7 mmol) and the catalyst precursor (0.07 mmol) were charged in a high-pressure glass vessel. The vessel was sealed in a glovebox under nitrogen atmosphere. The glass vessel was immersed into a furnace at the desired reaction temperature and time with continuous stirring. After reaction, the reactor was cooled down to room temperature and CH₂Cl₂ containing dodecane as the internal standard were added into the system. The reactor was sealed and transferred to the furnace again at 70 °C for 20 min, in order to wash all products into CH₂Cl₂ solution. Finally, the reaction mixture was transferred to a volumetric flask and diluted to 10 mL.

The CH₂Cl₂ solution was passed by a filter to remove any solid. The products were qualified with gas-chromatography mass spectrometer (GC-MS) on an Agilent 7890-5975C and quantified by gas chromatograph (GC) on an Agilent GC-7890 equipped with a HP-5 capillary column and flame ionization detector (FID). The conversion of stearic acid was determined

on an Agilent HPLC-1200 with an Agilent ZORBAX C18 column using methanol and water as mobile phase.

2.3 Ni nanoparticles isolation

After the catalytic deoxygenation of stearic acid was carried out over 1 mol% Ni(OAc)₂ at 350 °C for 2 h, the reaction mixture was collected and centrifuged at 60 °C to remove stearic acid. The solid was then washed with CH₂Cl₂ for three times to remove additional stearic acid and dried for use.

2.4 Characterization

X-ray diffraction (XRD) analysis was performed on a Bruker D8 Advanced Diffractometer with Cu K α ($\lambda = 1.5418 \text{ \AA}$) at 40 kV. Transmission electronic microscopic (TEM) images were obtained on a JEOL 2100 under 200 kV. Thermogravimetric analysis (TGA) was carried out on a Shimadzu DTG-60AH with a nitrogen stream of 100 mL/min from 25 °C to 1000 °C at a rate of 10 °C/min. Fourier transformed infrared (FT-IR) spectra was determined on a Bio-Rad FTS-3500 ARX instrument. X-ray absorption spectroscopy (XAS) on the Ni K-edge was measured at the 1W1B beamline at the Beijing Synchrotron Radiation Facility (BSRF) in transmission mode using ion chamber detector to collect data. Ni foil, NiO and all Ni precursors were measured as standards.

3. Results and discussion

3.1 Catalysts screening

The deoxygenation process of stearic acid at 350 °C for 2 h under a nitrogen atmosphere did not occur in the absence of a catalyst—only 4.8% products were generated, among which a majority (78%) was heavy products (mainly stearone and 2-C19-one). At higher temperature, the auto-decomposition of stearic acid was more pronounced, but the selectivity was largely directly to cracking products (C₈-C₁₆) (Table S1). The catalytic activity of a series of metal acetate salts was evaluated as pre-catalysts for the reaction as shown in Table 1 (entries 2-12). These acetate salts were selected as they are all easily available and more importantly, acetate represents the simplest fatty acid carboxylate so that the anion effect is minimized. The catalytic performance of these 11 acetate salts differed drastically from each other, with Ni(OAc)₂ being the most effective and NaOAc/Ca(OAc)₂ being almost inert. TGA results (Fig. S1a) revealed that all salts decomposed under reaction conditions except NaOAc and Ca(OAc)₂ which only decomposed above 400 °C. The latter two salts, maintained their original state in the reaction, can hardly catalyze the deoxygenation of stearic acid. The other acetate salts decomposed at 350 °C to form heterogeneous catalytic systems. Ag, Pd and Rh acetate salts decomposed into metallic metals according to the weight of the residues obtained from TGA results, but these metal catalysts were not effective in the reaction. For example, only 10.1% of products were obtained over Pd(OAc)₂, although high activity of supported Pd(0) catalyst has been achieved in previous reports. This may result from the large size and low metal dispersion of Pd in the

Table 1. Performance of screened catalysts in the deoxygenation of stearic acid without H₂^a

$$\text{C}_{17}\text{H}_{35}\text{COOH} \longrightarrow \text{C}_8\text{-C}_{16} + \text{C}_{17}\text{H}_{34} + \text{C}_{17}\text{H}_{36} + \text{CH}_3\text{-}\overset{\text{O}}{\parallel}\text{C}\text{-C}_{17}\text{H}_{35} + \text{C}_{17}\text{H}_{35}\text{-}\overset{\text{O}}{\parallel}\text{C}\text{-C}_{17}\text{H}_{35}$$

Cracking
Heptadecene
Heptadecane
2-C19-one
Stearone

Entry	Catalyst	GC yield / % ^b					HPLC Conv. / % ^c	
		Cracking product	Heptadecene	Heptadecane	Stearaldehyde	Heavy product		Total
1	Blank	0.7	0.2	< 0.1	0.1	3.8	4.8	7.4
2	NaOAc	-	-	0.2	-	0.2	0.4	2.9
3	Ca(OAc) ₂	1.7	1.0	-	-	1.2	3.9	4.0
4	Cu(OAc) ₂	1.5	0.5	1.5	-	0.2	3.7	11.3
5	Zn(OAc) ₂	1.8	< 0.1	0.1	-	3.5	5.4	23.3
6	Mn(OAc) ₂	2.3	0.3	0.3	-	15.6	18.4	26.5
7	Co(OAc) ₂	1.8	0.6	1.5	-	12.8	16.7	31.3
8	Ni(OAc) ₂	2.3	22.4	18.9	-	13.8	57.4	72.0
9	AgOAc	3.5	1.4	3.6	-	1.5	10.0	12.7
10	Pd(OAc) ₂	1.9	5.7	1.3	-	1.2	10.1	16.7
11	[Rh(OAc) ₂] ₂	2.5	3.9	1.0	-	0.6	8.0	9.6
12	Au(OAc) ₃	2.7	0.4	0.4	-	2.0	5.5	11.6
13	Ni(acac) ₂	3.8	21.4	18.4	-	13.7	57.3	68.8
14	Ni(NO ₃) ₂	8.9	14.6	13.1	-	10.9	47.5	62.6
15	NiCl ₂	0.5	4.6	5.5	-	0.6	11.2	13.5
16	NiSO ₄	1.3	-	1.0	-	0.1	2.4	4.2
17	Ni-isolated ^d	5.1	19.6	29.6	-	2.0	56.3	58.2

^a Reaction conditions: stearic acid (200 mg); metal salt (10 mol%); T = 350 °C; t = 2 h. ^b Determined by GC and calculated according to effective carbon number with dodecane as internal standard. Cracking: C8-C16 alkenes and alkanes; Heavy product: 2-C19-one and stearone; -: not detected. ^c Determined by HPLC. ^d Ni NPs isolated from catalytic system after reaction (Ni(OAc)₂ as pre-catalyst).

present study as the metal dispersion will affect the deoxygenation activity of fatty acid considerably.⁴¹ Mn(OAc)₂ and Co(OAc)₂ exhibited slightly better activity than Cu, Zn salts, enabling 18.4% and 16.7% product yield respectively, but these two catalysts led to the formation of a considerable portion of undesired cracking and heavy products (ca. 97% and 87% combined selectivity in Mn(OAc)₂ and Co(OAc)₂, respectively) such as 2-C₁₉-one and stearate ketone (entries 4 - 7). Among all the catalysts screened, Ni(OAc)₂ was the most active for the deoxygenation of stearic acid with 72.0% conversion and 57.4% product yield, among which 72% belongs to C₁₇ hydrocarbons (Table 1, entry 8). The exceptional performance of Ni(OAc)₂ prompted us to examine other nickel salts such as Ni(NO₃)₂, Ni(acac)₂, NiCl₂ and NiSO₄ as pre-catalysts under identical conditions (Table 1, entries 13-16). Ni(NO₃)₂ and Ni(acac)₂ were similarly active compared with Ni(OAc)₂, achieving 62.6% and 68.8% stearic acid conversion with 47.5% and 57.3% product yield, respectively. On the other hand, NiCl₂ and NiSO₄ exhibited little catalytic activity. We further analyzed these four Ni salts using TGA. Similar to Ni(OAc)₂, Ni(acac)₂ and Ni(NO₃)₂ fully decomposed before 400 °C, whereas NiCl₂ and NiSO₄ were stable and decomposed only at a much higher temperature (ca. 800 °C, Fig. S1b). These TGA results indicated that Ni(OAc)₂, Ni(acac)₂ and Ni(NO₃)₂ were decomposed under the applied reaction conditions, while NiCl₂ and NiSO₄ remained in the form of a metal salt.

From these observations, it was clear that Ni²⁺ in the salt form was inactive for the H₂ free deoxygenation reaction of fatty acid, and decomposed Ni salts were the active catalytic species. TGA results, however, could not reveal whether the decomposed Ni species was metallic Ni or NiO. Noteworthy, Ni species were exposed to an inert atmosphere in TGA whereas Ni species were in contact with fatty acids and their derivatives during the reaction.

Several combinations between Ni(OAc)₂ and other metal acetate as the pre-catalysts were further tested (Table S2), but the product yield was not enhanced. As such, further studies were focused on single component Ni salts.

3.2 Active species identification

Several characterization techniques were performed to identify the true catalytic active species. XRD patterns of different nickel salts with stearic acid before and after reaction are shown in Fig. 1a and Fig. S2. Before reaction, 10 mol% nickel salts and stearic acid were mixed together under grinding conditions and then used for XRD characterization. The results in Fig. S2a suggested that these samples all exhibited the peaks belong to stearic acid. The spectra also showed the peaks from nickel salts, although these peaks were very weak and difficult to identify due to the complexity and strong intensity of peaks from stearic acid. After reaction, the peaks from Ni(OAc)₂, Ni(acac)₂ and Ni(NO₃)₂ salts disappeared (Fig. S2b) whereas the diffraction peak of metallic Ni (at ca.

44.6 °) appeared in the enlarged XRD patterns (Fig. 1a). Plausibly, these Ni salts decomposed and were reduced to Ni(0) over reducing species such as CO and H₂ generated in the reaction. Not unexpected, the peak belonging to Ni(0) was not observed in catalytic systems where NiCl₂ and NiSO₄ were used as pre-catalysts, in agreement with TGA results.

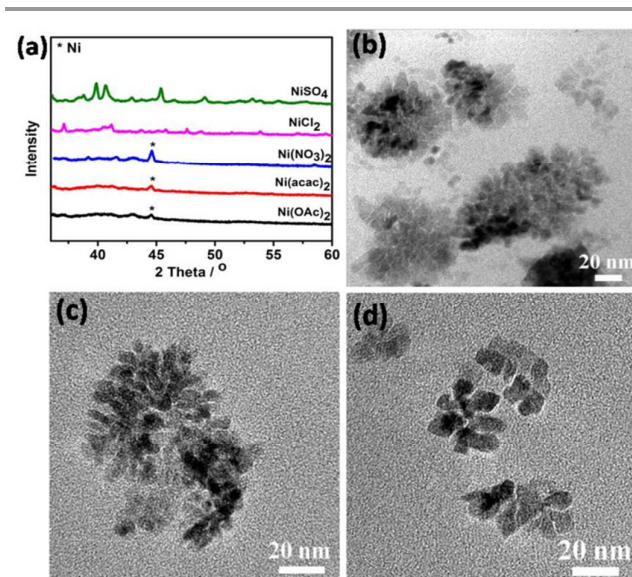


Fig. 1 (a) Typical XRD patterns of stearic acid and nickel salts after reaction (enlarge spectra); and TEM images of (b) Ni(OAc)₂, (c) Ni(acac)₂ and (d) Ni(NO₃)₂ catalytic systems after reaction.

Besides XRD, XAS was also applied to investigate the state of nickel after reaction. The samples were sealed in a chamber with Kapton film windows under Ar protection in a glovebox after reaction. In agreement with XRD data, metallic nickel was observed in the Ni(OAc)₂, Ni(acac)₂ and Ni(NO₃)₂ systems (Fig. S3a), whereas NiCl₂ and NiSO₄ still maintained the same valence state as the precursor (Fig. S3b and Fig. S3c). Nickel oxide was also observed in the Ni(OAc)₂, Ni(acac)₂ and Ni(NO₃)₂ systems, which indicated some of the surface Ni was oxidized during the sample preparation process.

Since XRD patterns and XAS results both suggested the existence of metallic Ni after reaction, TEM was applied to characterize the size and morphology of these particles. TEM images revealed the formation of highly dispersed, 8-10 nm nanoparticles during the reaction in the Ni(OAc)₂, Ni(acac)₂ and Ni(NO₃)₂ catalytic systems (Fig. 1b-1d). The nanoparticles in the Ni(OAc)₂ catalyst system have been further analyzed with TEM-EDX and TEM-EDX mapping, confirming the existence of Ni in these nanoparticles (Fig. S4a). On the other hand, only bulk structures of aggregates were observed in the NiCl₂ and NiSO₄ systems. TEM-EDX mapping exhibited approximately the same atomic ratio between Ni:Cl and Ni:S as nickel precursors in these two samples, respectively. This suggested that these two salts did not decompose under the catalytic conditions (Fig. S4b and Fig. S4c). Combining TGA, XRD, XAS and TEM analysis, Ni salt precursors are inactive in the reaction. Instead,

in situ formed, nanosized Ni metal particles were responsible for the high activity for the H₂-free deoxygenation of stearic acid. We further isolated the *in situ* formed Ni NPs after the reaction (Ni(OAc)₂ as pre-catalyst) for a second batch of reaction. The product yield remained essentially the same while the stearic acid conversion slightly dropped (Table 1 entry 17). Interestingly, these Ni nanoparticles were unsupported and unprotected by any additional stabilizer, yet they were small in size, stable and catalytically active under harsh conditions. We propose that stearic acid acted as a stabilizer and ligand for the Ni nanoparticles. Noteworthy the use of fatty acids as surfactant for the synthesis of different kinds of nanoparticles has been previously reported, despite different synthetic conditions.⁴²⁻⁴⁴

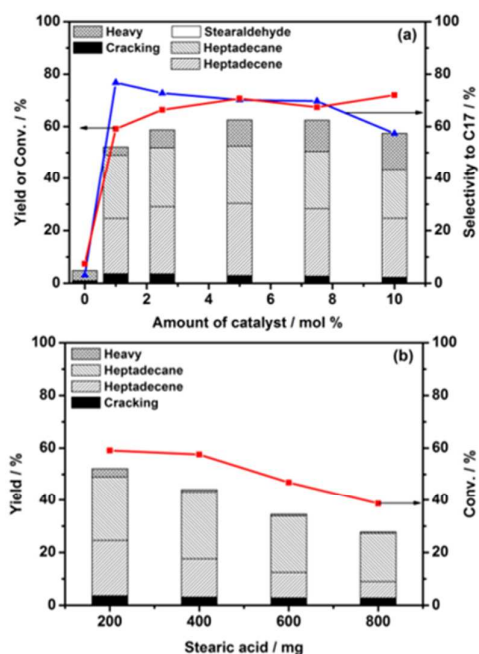


Fig. 2 (a) Effects of catalyst loading on catalytic activity; reaction conditions: stearic acid (200 mg); catalyst: Ni(OAc)₂; T = 350 °C; t = 2 h. (b) Effects of substrate amount on catalytic activity; reaction conditions: substrate, stearic acid; Ni(OAc)₂ (0.007 mmol); T = 350 °C; t = 2 h. Note: The activity data of blank was taken from Table 1, entry 1; the 10 mol% catalyst amount and 200 mg of stearic acid was taken from Table 1, entry 8.

3.3 Catalyst loading test

Next, we tested the catalytic performance of the Ni(OAc)₂ with varying loadings. As illustrated in Fig. 2a, the deoxygenation process can hardly occur without catalyst (the yield of heptadecene and heptadecane was less than 1%). However, when 1 mol% of Ni(OAc)₂ was added into the system, the conversion of stearic acid increased dramatically to 59% and the selectivity to C17 hydrocarbons increased from 3% to 77%. This result indicated the necessity of the catalyst to improve the deoxygenation activity and selectivity to C17 hydrocarbons. With an increase of the catalyst amount from 1 mol% to 5 mol%, the conversion of stearic acid increased steadily from 59% to 71%. This number maintained almost unchanged when the catalyst loading exceeded 5 mol%. Reducing the catalyst

loading below 1 mol% while maintain the same stearic acid amount was not practical as the measurement of small quantities of $\text{Ni}(\text{OAc})_2$ could not be accurately determined. Therefore, the amount of substrate was increased, while keeping the $\text{Ni}(\text{OAc})_2$ amount constant to reduce the catalyst loading (Fig. 2b). The conversion decreased with the increase of stearic acid amount. Nevertheless, even with 0.25 mol% $\text{Ni}(\text{OAc})_2$, 39% of the stearic acid could be converted with 64% selectivity towards C17 hydrocarbons. The activity of Ni nanoparticles formed *in situ*, based on C17 hydrocarbon yields, was calculated to be $14.5 \text{ mol} \cdot \text{mol}^{-1} \cdot \text{h}^{-1}$, which was two orders of magnitude higher than that obtained in Al_2O_3 supported nickel catalysts carried out under He ($0.079 \text{ mol} \cdot \text{mol}^{-1} \cdot \text{h}^{-1}$).⁴⁰ Furthermore, this activity was 30 times higher than supported nickel catalysts operated under H_2 atmosphere ($0.48 \text{ mol} \cdot \text{mol}^{-1} \cdot \text{h}^{-1}$).²⁵ These results suggested that the *in situ* formed Ni nanoparticles were superior to supported Ni catalysts in the deoxygenation of stearic acid, presumably due to the very small size of the Ni NPs in the system.

3.4 Kinetic study

Since 1 mol% of $\text{Ni}(\text{OAc})_2$ exhibited the highest selectivity to deoxygenation products at a relatively high conversion, it was

used in the kinetic study. The product yields with respect to reaction time at different reaction temperatures was determined (Fig. 3a). As discussed previously, the metallic nickel nanoparticles formed during the reaction catalyzed the stearic acid deoxygenation, however, no induction period can be observed from the kinetic curve and suggested that the formation of nickel nanoparticles was very fast. According to previous reports,^{35,45} the deoxygenation of stearic acid was considered as a first order reaction with respect to liquid products. As expected, the reaction rate increased with reaction temperature and the rate constants of the deoxygenation at each temperature were summarized in Table S3. Each temperature followed a similar trend between product yield and time, in which at the beginning of the reaction the yield increased with time and then reached a steady state. Higher temperatures increased the reaction rate and a shorter time was required to reach a steady state. Higher temperatures also led to lower final product yields. For example, the catalytic reactions carried out at 370 °C and 390 °C could reach the steady state within 60 and 30 min, respectively, but only 45% and 42% product yields were achieved.

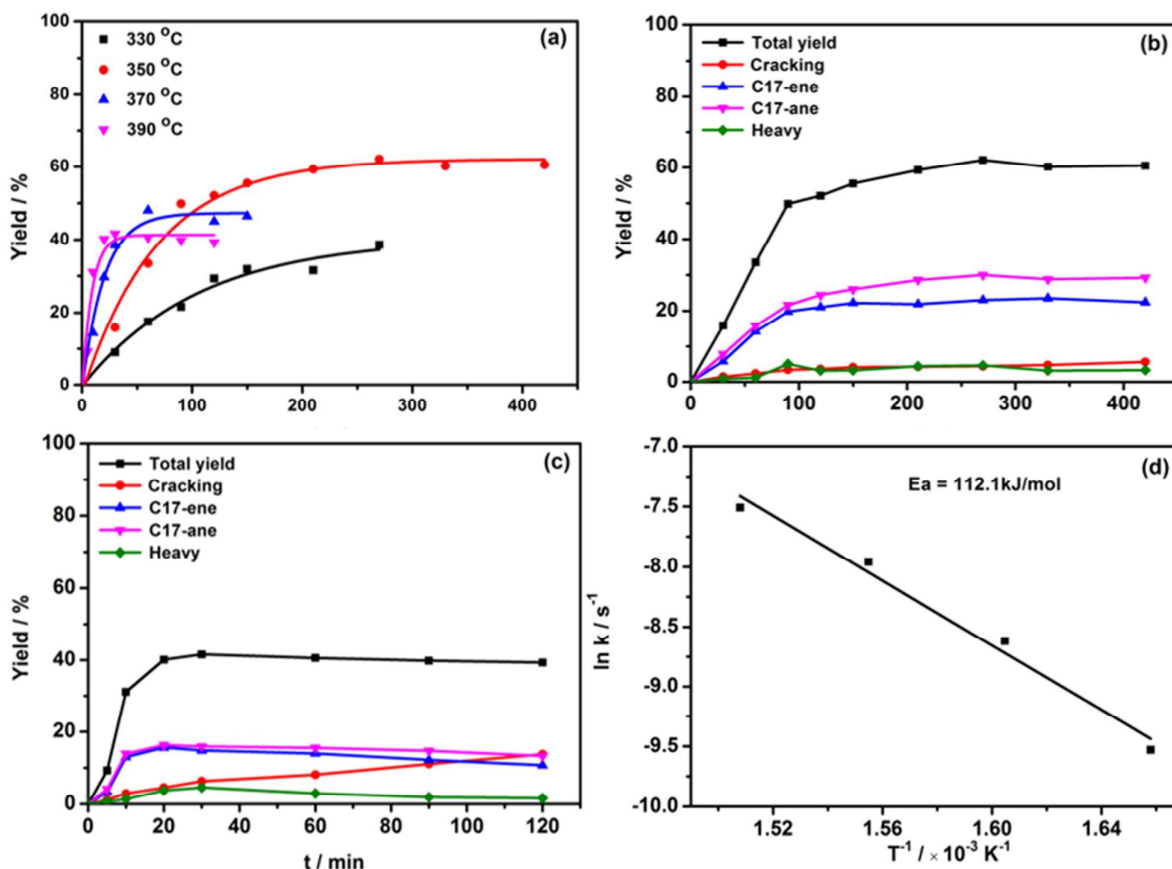


Fig. 3 The variation of product yields with time at different temperatures. (a) Total product yield at each temperature; (b) Product yield with time at 350 °C; (c) Product yield with time at 390 °C; (d) Arrhenius plot of rate constants and temperature.

To better understand the reaction sequence, the yield of each product as a function of time was analyzed. At 330 °C and 350 °C, all products followed the same trend as the total product yield in the entire duration (Fig. S5a and Fig. 3b). When reaction was conducted at 370 °C, all products showed similar trend in the first 60 min. Afterwards, the total product yield kept unchanged while the increase in the cracking product yield was observed at the expense of heavy products (Fig. S5b). This phenomenon was particularly obvious in catalytic system at 390 °C after 30 min (Fig. 3c). The increase in cracking product yield from heavy ones was more likely to produce carbon coking on catalysts and cause catalyst deactivation, which may result in the lower final yields at 370 °C and 390 °C.

The variation of the rate constants with temperature (Table S3) followed the Arrhenius Equation prediction. The apparent activation energy of this reaction over nickel catalyst was 112.1 kJ/mol, based on fitting the parameters with a linear correlation of $\ln k \sim 1/T$ (Fig. 3d). The activation energy of this catalytic system was significantly lower than supported nickel catalysts employed under hydrogen atmosphere, suggesting again the much higher efficiency of the *in situ* formed Ni nanoparticle catalysts in the present system.⁴⁵

3.5 Reaction pathway

Since stearate ketone can be obtained from the decarboxylation of stearic anhydride and stearone was detected in current catalytic system, stearic anhydride was proposed as an intermediate of the deoxygenation process of stearic acid as reported in literature.⁴⁶ When stearic anhydride was used as the substrate in the absence of catalyst, the major product was the stearate ketone and stearic acid. Only trace amounts of C17 hydrocarbons were observed (Table 2, entry 1). These results indicated that the formation of stearic acid and stearate ketone from anhydride can be proceeded readily without catalyst. When 1 mol% of the nickel catalyst was added into the reaction system, the yield of C17 hydrocarbons increased sharply within 10 min. The yield of heptadecene and heptadecane increased to 15.6% and 22.2%, respectively, when further prolonging the reaction to 30 min, which is much higher than that obtained from stearic acid under the same reaction conditions (Table 2, entries 2-4). This phenomenon suggested that heptadecene and heptadecane

can be directly produced from stearic anhydride without being hydrolyzed to stearic acid. The gas phase product was also analyzed to provide additional information on the reaction pathway. After carrying out the deoxygenation reaction at 350 °C with stearic acid as substrate for 2.5 h, the gas products were collected and examined with FT-IR. As expected, both CO₂ and CO peaks appeared in the spectra (Fig. S6) with an approximate concentration ratio of 1:10. At 350 °C, the reverse water gas shift (RWGS) reaction was thermodynamically unfavorable with $\Delta G = 16.7$ kJ/mol, suggesting CO was mainly formed from a decarbonylation process rather than from the RWGS. On the contrary, the conversion of CO to CO₂ through the water gas shift reaction was likely to occur under applied conditions. In the literature, it was proposed that alkane was mainly generated by decarboxylation,⁴⁶ however, it appears heptadecane in our system is generated mainly via a two-stage route starting from stearic anhydride. The first stage was the hydrogenation of stearic anhydride to form stearaldehyde which subsequently underwent a decarbonylation reaction to heptadecane. H₂ was confirmed to exist in system through the processes of cracking, dehydrogenation and water gas shift reaction under N₂ atmosphere.^{38,47} Further, stearic aldehyde was also detected (Table 1, entry 1 and Table 2, entry 1) and provided additional evidence for the proposed pathway. Combined the reaction network of stearic acid deoxygenation over Ni(OAc)₂ as pre-catalyst under inert gas atmosphere is illustrated in Fig. 4.

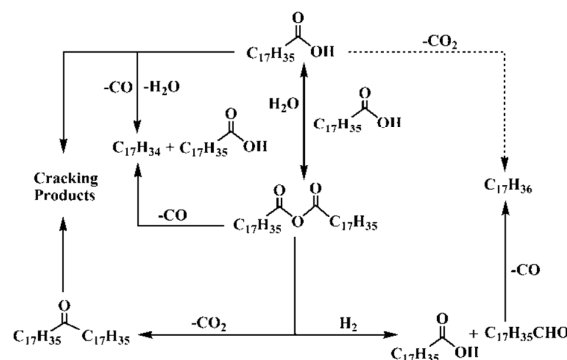


Fig. 4 Reaction pathway of stearic acid under N₂ atmosphere. The dot line indicated the limited reaction pathway.

Table 2. Stearic anhydride as substrate for the deoxygenation process^a

Entry	Substrate	Catalyst	Time / min	Yield / % ^b					
				Cracking	Heptadecene	Heptadecane	Stearic aldehyde	Heavy	Stearic acid ^c
1	Stearic anhydride	-	30	0.88	1.24	0.83	0.03	10.3	37.4
2	Stearic anhydride	Ni(OAc) ₂	10	0.87	8.12	11.3		10.5	42.4
3	Stearic anhydride	Ni(OAc) ₂	30	1.89	15.6	22.2		10.9	29.5
4	Stearic acid	Ni(OAc) ₂	30	1.47	5.82	7.77		0.81	-

^a Reaction conditions: substrate (200 mg); catalyst amount (1 mol%); T = 350 °C. ^b Determined by GC. ^c Determined by HPLC.

3.6 Recyclability

As shown by entry 17 in Table 1, the isolated Ni nanoparticles after reaction was reused as catalyst and the catalytic performance was almost same to the Ni(OAc)₂. However, it is difficult to further continue the recycling due to the very small amount of Ni used (< 0.5 mg). To conveniently assess the long term stability and recyclability of the catalyst, 200 mg of stearic acid was re-added to the system after a 2 h reaction at 350 °C without separation, and then kept under the same conditions for another 2 h. After four repeats (Fig. 5), the activity of nanoparticles could be maintained at around 52% ~ 55% of yield without any loss. As such these Ni nanoparticles formed *in situ* were very active and stable for the deoxygenation of stearic acid to produce liquid hydrocarbons.

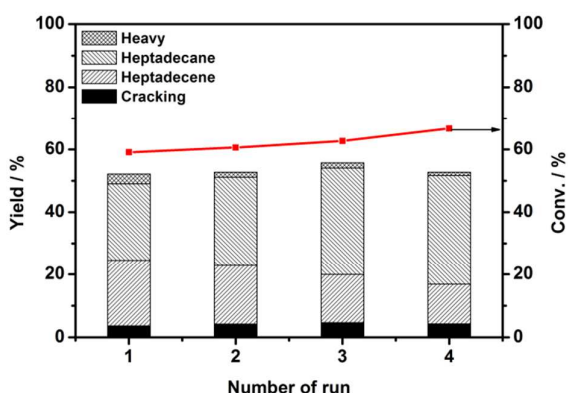


Fig. 5 Stability study of nickel catalyst for the stearic acid deoxygenation. Reaction conditions: substrate, stearic acid; Ni(OAc)₂ (1 mol%); T = 350 °C, t = 2 h.

3.7 Substrate scope

Finally, deoxygenation of free fatty acids bearing different carbon chain length and double bonds were studied over Ni(OAc)₂ as pre-catalyst at 350 °C for 4.5 h without H₂ and

solvent. There was a clear trend that a decrease in deoxygenation catalytic activity was observed with the decrease of carbon number in the fatty acid. This observation was inconsistent with previous reports carried out over Pd/C catalyst indicating that the carbon chain length did not have any effect on the activity.^{48,49} This could be rationalized by considering that the real catalyst was formed *in situ* under interaction with the fatty acid substrate. When different free fatty acids were used, the Ni nanoparticles formed *in situ* varied from one another as the surfactant properties of the system were altered, which influenced the size and morphology of the nanoparticles,⁵⁰ and ultimately the deoxygenation activity. For unsaturated feedstocks such as oleic acid and linoleic acid, the deoxygenation activity was low, which was in agreement with the literature that the adsorption of double bonds onto metal catalysts inhibit the deoxygenation reaction.^{47,51} Encouragingly, Ni(OAc)₂ was also applicable in deoxygenating tristearin, which was the major component of oil and fats (Table 3, entry 8), with comparable yields of C16-acid and C18-acid substrates.

Conclusions

Highly effective deoxygenation of stearic acid into alkanes and other products was successfully achieved over a small loading of commercially available and cheap Ni(OAc)₂ as pre-catalyst under solvent and hydrogen-free conditions. The real catalytic active species were Ni nanoparticles formed *in situ*, with fatty acids acting as a stabilizer and capping agent. These nanoparticles are much more active than supported Ni catalysts in previous reports and can be reused for at least four times without any loss in activity. A new reaction pathway for alkane formation via the intermediate of stearic anhydride under inert gas was proposed. This study provides an alternative way for the production of transportation fuels featured by low cost, high activity and stability of the catalyst.

Table 3. Catalytic activity of Ni(OAc)₂ on different substrates^a

Entry	Substrate	Yield / % ^b							Conversion / % ^c
		Cracking	C _{n-1} -ene	C _{n-1} -ane	Heavy	Palmitic acid ^c	Stearic acid ^c	Total	
1	C18-acid	4.40	23.0	30.0	4.64	-	-	62.1	67.5
2	C16-acid	2.83	19.7	18.8	4.97	-	-	46.3	53.1
3	C12-acid	1.71	5.85	3.72	4.63	-	-	15.9	15.3
4	C10-acid	0.90	1.16	1.17	1.09	-	-	4.32	3.18
5	Oleic acid	2.41	-	25.6	-	-	-	28.0	73.9
6	Linoleic acid	1.83	-	12.9	-	-	-	14.7	32.8
7	Methyl stearate	3.38	-	-	-	-	-	3.38	5.36
8	Tristearin	14.2	7.14	13.6	2.30	6.10	16.0	59.7	-

^a Reaction conditions: substrate (0.7 mmol); Ni(OAc)₂ (1 mol%); T = 350 °C; t = 4.5 h. ^b Determined by GC. ^c Determined by HPLC.

Acknowledgements

We thank the MOE Tier-1 project (WBS R-279-000-438-112), Natural Science Foundation of China (21173009, 21222306) and 973 Project (2011CB201402, 2013CB933100) for the financial support. W. J. Li thanks the China Scholarship Council for the fellowship. We also thank Dr. Kylie Luska for the proof reading.

References

- P. Gallezot, *Chem. Soc. Rev.*, 2012, **41**, 1538.
- C.-H. Zhou, X. Xia, C.-X. Lin, D.-S. Tong, J. Beltramini, *Chem. Soc. Rev.*, 2011, **40**, 5588.
- M. Besson, P. Gallezot, C. Pinel, *Chem. Rev.*, 2014, **114**, 1827.
- J. Zhang, H. Asakura, J. van Rijn, J. Yang, P. Duchesne, B. Zhang, X. Chen, P. Zhang, M. Saeys and N. Yan, *Green Chem.*, 2014, **16**, 2432.
- X. Chen, S. L. Chew, F. M. Kerton and N. Yan, *Green Chem.*, 2014, **16**, 2204.
- R. W. Gosselink, S. A. Hollak, S. W. Chang, J. van Haveren, K. P. de Jong, J. H. Bitter and D. S. van Es, *ChemSusChem*, 2013, **6**, 1576.
- O. O. James, S. Maity, M. A. Mesubi, L. A. Usman, K. O. Ajanaku, T. O. Siyanbola, S. Sahu and R. Chaubey, *Int. J. Energ. Res.*, 2012, **36**, 691.
- N. N. A. N. Yusuf, S. K. Kamarudin and Z. Yaakub, *Energ. Convers. Manage.*, 2011, **52**, 2741.
- M. K. Lam, K. T. Tan, K. T. Lee and A. R. Mohamed, *Renew. Sust. Energ. Rev.*, 2009, **13**, 1456.
- M. Snåre, I. Kubičková, P. Mäki-Arvela, D. Chichova, K. Eränen and D. Y. Murzin, *Fuel*, 2008, **87**, 933.
- S. Lestari, P. Mäki-Arvela, J. Beltramini, G. Q. Lu and D. Y. Murzin, *ChemSusChem*, 2009, **2**, 1109.
- M. A. H. Fangrui Ma, *Bioresour. Technol.*, 1999, **70**, 1.
- C. Zhao, T. Brück and J. A. Lercher, *Green Chem.*, 2013, **15**, 1720.
- S. P. Singh and D. Singh, *Renew. Sust. Energ. Rev.*, 2010, **14**, 200.
- J. Dupont, P. A. Z. Suarez, M. R. Meneghetti and S. M. P. Meneghetti, *Energ. Environ. Sci.*, 2009, **2**, 1258.
- N. Taufiqirrahmi and S. Bhatia, *Energ. Environ. Sci.*, 2011, **4**, 1087.
- D. Verma, R. Kumar, B. S. Rana and A. K. Sinha, *Energ. Environ. Sci.*, 2011, **4**, 1667.
- J. A. Botas, D. P. Serrano, A. García, J. de Vicente and R. Ramos, *Catal. Today*, 2012, **195**, 59.
- E. Santillan-Jimenez and M. Crocker, *J. Chem. Technol. Biotechnol.*, 2012, **87**, 1041.
- W. Han, H. Sun, Y. Ding, H. Lou and X. Zheng, *Green Chem.*, 2010, **12**, 463-467.
- R. W. Gosselink, D. R. Stellwagen and J. H. Bitter, *Angew. Chem. Int. Ed. Engl.*, 2013, **52**, 5089.
- B. Peng, C. Zhao, S. Kasakov, S. Foraita and J. A. Lercher, *Chem. Eur. J.*, 2013, **19**, 4732.
- C. Wang, Z. Tian, L. Wang, R. Xu, Q. Liu, W. Qu, H. Ma and B. Wang, *ChemSusChem*, 2012, **5**, 1974.
- V. A. Yakovlev, S. A. Khromova, O. V. Sherstyuk, V. O. Dundich, D. Y. Ermakov, V. M. Novopashina, M. Y. Lebedev, O. Bulavchenko and V. N. Parmon, *Catal. Today*, 2009, **144**, 362.
- B. Peng, X. Yuan, C. Zhao and J. A. Lercher, *J. Am. Chem. Soc.*, 2012, **134**, 9400.
- A. S. Berenblyum, R. S. Shamsiev, T. A. Podoplelova and V. Y. Danyushevsky, *Russ. J. Phys. Chem. A*, 2012, **86**, 1199.
- Sun, K.; Wilson, A. R.; Thompson, S. T.; Lamb, H. H. *ACS Catal.* **2015**, **5**, 1939.
- Kandel, K.; Frederickson, C.; Smith, E. A.; Lee, Y. J.; Slowing, I. I. *ACS Catal.* **2013**, **3**, 2750.
- Yang, Y.; Ochoa-Hernández, C.; de la Peña O'Shea, V. A.; Coronado, J. M.; Serrano, D. P. *ACS Catal.* **2012**, **2**, 592.
- P. Mäki-Arvela, M. Snåre, K. Eränen, J. Myllyoja and D. Y. Murzin, *Fuel*, 2008, **87**, 354 3.
- H. Bernas, K. Eränen, I. Simakova, A. R. Leino, K. Kordás, J. Myllyoja, P. Mäki-Arvela, T. Salmi and D. Y. Murzin, *Fuel*, 2010, **89**, 2033.
- E. W. Ping, R. Wallace, J. Pierson, T. F. Fuller and C. W. Jones, *Microporous Mesoporous Mater.*, 2010, **132**, 174.
- Gosselink, R. W.; Xia, W.; Muhler, M.; de Jong, K. P.; Bitter, J. H. *ACS Catal.* **2013**, **3**, 2397.
- J. Fu, X. Lu and P. E. Savage, *ChemSusChem*, 2011, **4**, 481.
- J. Fu, X. Y. Lu and P. E. Savage, *Energ. Environ. Sci.*, 2010, **3**, 311.
- T. Morgan, E. Santillan-Jimenez, A. E. Harman-Ware, Y. Ji, D. Grubb and M. Crocker, *Chem. Eng. J.*, 2012, **189-190**, 346.
- J. A. Botas, D. P. Serrano, A. García and R. Ramos, *Appl. Catal., B*, 2014, **145**, 205.
- T. Morgan, D. Grubb, E. Santillan-Jimenez and M. Crocker, *Top. Catal.*, 2010, **53**, 820.
- S. Idesh, S. Kudo, K. Norinaga and J. Hayashi, *Energy Fuels*, 2013, **27**, 4796.
- M. Snåre, I. Kubickova, P. Mäki-Arvela, K. Eränen and D. Y. Murzin, *Ind. Eng. Chem. Res.*, 2006, **45**, 5708.
- I. Simakova, O. Simakova, P. Mäki-Arvela, A. Simakov, M. Estrada and D. Y. Murzin, *Appl. Catal., A*, 2009, **355**, 100.
- H. Basit, A. Pal, S. Sen and S. Bhattacharya, *Chem. Eur. J.*, 2008, **14**, 6534.
- Y. C. Nikhil, R. Jana, and X. G. Peng, *Chem. Mater.*, 2004, **16**, 3931.
- M. V. Kovalenko, M. I. Bodnarchuk, R. T. Lechner, G. Hesser, F. Schaffler and W. Heiss, *J. Am. Chem. Soc.*, 2007, **129**, 6352.
- P. Kumar, S. R. Yenumala, S. K. Maity and D. Shee, *Appl. Catal., A*, 2014, **471**, 28.
- S. A. W. Hollak, J. H. Bitter, J. Haveren, K. P. de Jong and D. S. van Es, *RSC Adv.*, 2012, **2**, 9387.
- J. G. Immer, M. J. Kelly and H. H. Lamb, *Appl. Catal., A*, 2010, **375**, 134.
- I. Simakova, O. Simakova, P. Mäki-Arvela and D. Y. Murzin, *Catal. Today*, 2010, **150**, 28.
- S. Lestari, P. Mäki-Arvela, I. Simakova, J. Beltramini, G. Q. M. Lu and D. Y. Murzin, *Catal. Lett.*, 2009, **130**, 48.
- X. Teng and H. Yang, *J. Mater. Chem.*, 2004, **14**, 774.
- S. A. W. Hollak, K. P. de Jong and D. S. van Es, *ChemCatChem*, 2014, **6**, 2648.

Effective deoxygenation of fatty acids over $\text{Ni}(\text{OAc})_2$ in the absence of H_2 and solvent

